Optik - International Journal for Light and Electron Optics 200 (2020) 163400

Contents lists available at ScienceDirect

Optik

journal homepage: www.elsevier.com/locate/ijleo

Original research article

Analysis of Bragg fiber waveguides having a defect layer for biosensing application

Ritesh Kumar Chourasia[a], Chandan Singh Yadav[b], Abhishek Upadhyay[b], Nitesh Kumar Chourasia[c], Vivek Singh[b,*]

[a] University Department of Physics, Lalit Narayan Mithila University, Darbhanga, 846003, India
[b] Department of Physics, Institute of Science, Banaras Hindu University, Varanasi, 221005, India
[c] School of Material Science and Technology, Indian Institute of Technology, BHU Varanasi, 221005, India

ARTICLE INFO

Keywords:
Bragg fiber waveguide
Transfer matrix method
Defect mode
High and low contrast cladding
Sensitivity

ABSTRACT

A novel hollow core Bragg fiber waveguides having a defect layer are proposed and analyzed theoretically for sensing application. Matching the electric and magnetic fields at various interfaces, a relation between fields of first layer with final layer has been stabilized; hence, the equations for reflectance and transmittance of proposed structure are derived. Due to periodicity of concentric cylindrical structure, a perfect photonic band gap is observed in considered wavelength range. The presence of defect layer in cylindrical periodic structure shows a peak corresponding to defect mode in perfect photonic band gap region. The full width at half maxima of this peak depends on the periodicity of the cladding layers. Also, the spectral position and shift of peak of defect mode depend on the angle of incidence of light, refractive index of core material and design wavelength of structure. Therefore, it is more appropriate to consider this peak of defect mode as sensing signal instead of considering whole photonic band gap as sensing signal.

1. Introduction

In conventional optical fiber waveguides, the propagation of the electromagnetic (EM) wave is taken place by the mechanism of total internal reflection (TIR). TIR in optical fiber waveguide is possible only when the refractive index (RI) of core is greater than the cladding RI. The high RI of core material causes various unwanted phenomena like dispersion, optical losses, non-linear effects, birefringence etc. These phenomena are minimized or removed by guiding the light in a hollow core waveguide. The hollow core waveguide can design by using multilayer concentric cylindrical fiber, where EM wave is guided by the Bragg reflections mechanism. In such type of fibers, the claddings are made by cylindrical shaped photonic crystals (dielectric mirrors). Fresnel's reflection through these alternating dielectric mirror causes constructive interference of the reflected wave and thus reflectance through such multilayer structure can be computed. Such multilayer reflections are analog to X ray scatterings in crystal structure and satisfied by the Bragg's law. Therefore such fibers with alternating permittivity of periodic multilayer claddings over a hollow or low refractive index core material are called Bragg fiber waveguide. The beginning of study about Bragg fiber waveguide structure was started in 1970's and further the concept of Bragg fiber waveguide was proposed in 1976 [1]. It was found that the Bragg fiber waveguide is allow only certain group of wavelengths to propagate in the core. Due to this specific property and being hallow core, such fiber waveguides are potentially useful in high power laser transmission where the nonlinear effects are mostly suppressed [2], bio and chemical sensing [3,4], telecommunication system [5], strain sensor [6], glucose sensor [7], optical de-multiplexers [8], omni reflector [9,10] etc.

* Corresponding author at: Department of Physics, Institute of Science, Banaras Hindu University, Varanasi, 221005, U.P., India.
E-mail address: viveks@bhu.ac.in (V. Singh).

https://doi.org/10.1016/j.ijleo.2019.163400
Received 7 August 2019; Received in revised form 4 September 2019; Accepted 9 September 2019

Nowadays researchers have taken keen interest to fabricate, explore and optimize the optical properties of planer photonic crystal which is also a periodic arrangement of high and low refractive index materials [11–13]. Further, to enhance the performance of these photonic crystals, they introduced a defect cavity in the structure [12] by breaking the symmetry of alternate multilayers. This introduced cavity in the multilayer planar structure behaves as Febry-Perot resonator cavity and a pass band (defect mode) is observed in existing photonic band gap (PBG) region. The basic difficulty of these planar photonic crystals are that they cannot be used as inline optical applications like high power laser systems, narrowband transmission filters etc. Keeping these things in mind, the above study is explored for periodic concentric cylindrical system having low refractive index core [14]. In this connection, to enhance the performance of these periodic multilayer cylindrical system, a hollow core Bragg fiber waveguide structure with a defect cavity has been introduced by the present investigators. Here the basic interest is to design and study theoretically a fiber waveguide to obtain 100% transmission window in PBG region.

Recently the researchers are involved to fabricate such periodic multilayer cylindrical structure by using drawing and rolling techniques [15,16]. In this technique, they first made preform of bilayers and then they draw into length using fiber drawing towers. This method can be used to make high contrast Bragg fibers where the low index layer is of polymer material and high index layer is of chalcogenide or perovskite material [3]. However, the rolling technique can be used to fabricate low contrast Bragg fiber waveguide i.e. both high and low index materials are of polymer film e.g. Polystyrene (PS) and Poly methyl methacrylate (PMMA) [4]. Both types of fiber waveguides can be used in sensing, telecommunication, or other optoelectronic applications. Due to their recent popularity, the present investigators are interested to explore the optical properties of both; high and low contrast Bragg fiber waveguides in presence of a defect layer. Since, in these waveguides the EM wave guidance occur through Bragg reflection mechanism and the defect peak appear due to the presence of defect cavity so it is logical to study the behavior of peak of defect mode in both high and low contrasts Bragg waveguides. Hence, in present paper hollow core Bragg fiber waveguides with defect cavity structure having high refractive index contrast of cladding layers (HRICCBF) and low refractive index contrast of cladding layers (LRICCBF) has been considered. The transfer matrix method is employed to study the propagation characteristic of proposed fiber waveguides. The paper is organized of as follows. In Section 2, basic equations and theoretical formulation of proposed cylindrical multilayer structures are given. The obtained results are discussed and illustrated in Section 3. A conclusion is drawn in Section 4.

2. Theoretical model and methods

The cross sectional view along the length of Bragg fiber waveguide with a defect layer is depicted in Fig. 1. In this figure, n_c, r_c shows the refractive index and radius of core while n_H, n_L and d_H, d_L shows the refractive indices and the respective thicknesses of high and low index layers, which form bilayer structure. Repeating these bilayers, multilayer Bragg fiber waveguide can be formed. In addition to this, a defect cavity having refractive index n_D and thickness d_D is introduced in the mid of the multilayer Bragg fiber waveguide which would act as Febry-Perot resonant cavity. In Bragg fiber waveguide the EM wave is supposed to be cylindrical due to the cylindrical symmetry of the proposed structure. The cylindrical wave is assumed to be diverging from the axis of symmetry $r = 0$, and then it strikes on the first cylindrical interface $r = r_0$. Now, applying transfer matrix method for the cylindrical waves [14,17] to calculate the reflectance of whole structure.

It is assumed that the temporal part of all the fields is exp(jωt). Hence the source free Maxwell's equations [18] are written as,

$$\nabla \times E = -j\omega H, \tag{1}$$

$$\nabla \times H = j\omega E. \tag{2}$$

For TE mode or H polarization in cylindrical coordinates (r,θ,z) [18], the non-zero fields E_z, H_θ, H_r satisfy the fallowing three equations in each layer,

$$\frac{1}{r}\frac{\partial E_z}{\partial \theta} = -j\omega\mu H_r, \tag{3a}$$

$$\frac{\partial E_z}{\partial r} = j\omega\mu H_\theta, \tag{3b}$$

$$\frac{\partial (rH_\theta)}{\partial r} - \frac{\partial H_r}{\partial \theta} = -j\omega\varepsilon r E_z. \tag{3c}$$

The governing differential equation for the tangential component of the electric field E_z can be written by using Eq. (3) as,

$$r\frac{\partial}{\partial r}\left(r\frac{\partial E_z}{\partial r}\right) - r^2\frac{1}{\mu}\frac{\partial \mu}{\partial r}\frac{\partial E_z}{\partial r} + \frac{\partial}{\partial \theta}\left(\frac{\partial E_z}{\partial \theta}\right) + \omega^2\varepsilon\mu r^2 E_z = 0. \tag{4}$$

Now, let us assume the field component $E_z = U(r)\Theta(\theta) = U(r)e^{im\theta}$, and the solution U is given as,

$$U(r) = C_1 J_m(kr) + C_2 Y_m(kr), \tag{5}$$

where C_1 and C_2 are constants, J_m is a Bessel function, Y_m is the Neumann function and k is the wave number in the material medium. The subscript m is the azimuthal mode number, which has been taken zero in this study. In the same manner, the tangential component of the magnetic field can be expressed as, $H_\theta = V(r)e^{im\theta}$, where $V(r)$ is given by,

$$V(r) = -jp(C_1 J_m'(kr) + C_2 Y_m'(kr)), \tag{6}$$

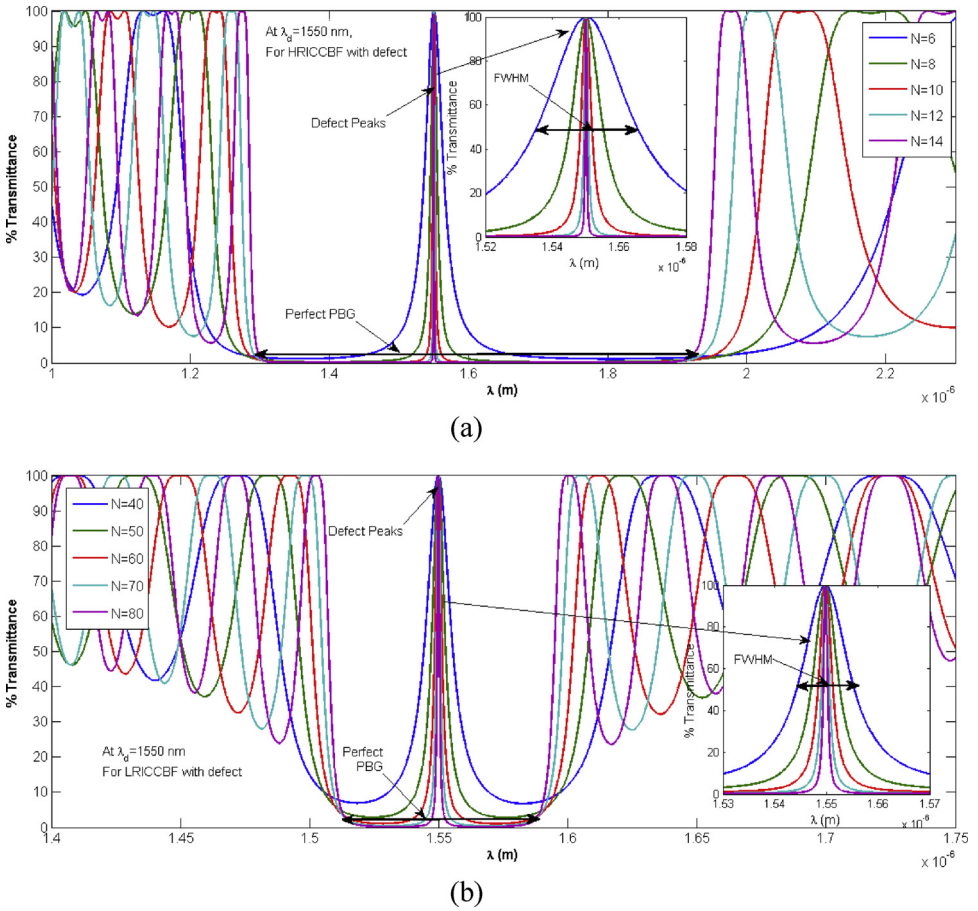

Fig. 1. Cross sectional view along the length of the hollow core Bragg fiber waveguide with a defect cavity.

where $p = \sqrt{\varepsilon/\mu}$ is the intrinsic admittance of the material medium.

A single layer matrix that relates the existing electric and magnetic fields at its two interfaces is constructed by using Eqs. (5) and (6) simultaneously. For instance, the matrix $\hat{T}_1$ for the first layer at interface ($r = r_0$ and r_1) is written as [17,19]

$$\begin{bmatrix} U(r_1) \\ V(r_1) \end{bmatrix} = \hat{T}_1 \begin{bmatrix} U(r_0) \\ V(r_0) \end{bmatrix}. \tag{7}$$

The component of the single layer matrix $\hat{T}_1 = \begin{bmatrix} t_{11} & t_{12} \\ t_{21} & t_{22} \end{bmatrix}$ can be written as

$$t_{11} = \frac{\pi}{2} k_1 r_0 [Y_m'(k_1 r_0) J_m(k_1 r_1) - J_m'(k_1 r_0) Y_m(k_1 r_1)], \tag{8a}$$

$$t_{12} = j\frac{\pi}{2}\frac{k_1}{p_1} r_0 [J_m(k_1 r_0) Y_m(k_1 r_1) - Y_m(k_1 r_0) J_m(k_1 r_1)], \tag{8b}$$

$$t_{21} = -j\frac{\pi}{2} k_1 r_0 p_1 [Y_m'(k_1 r_0) J_m'(k_1 r_1) - J_m'(k_1 r_0) Y_m'(k_1 r_1)], \tag{8c}$$

$$t^{22} = \frac{\pi}{2} k_1 r_0 [J_m(k_1 r_0) Y_m'(k_1 r_1) - Y_m(k_1 r_0) J_m'(k_1 r_1)], \tag{8d}$$

where $p_1 = \sqrt{\varepsilon_1/\mu_1}$. Eq. (8) shows that the matrix elements are strictly dependent on the radii of the two interfaces. Since, there is an additional defect layer which is introduced in the Bragg fiber waveguide, hence using Eq. (8) the transfer matrix for the defect layer will be constructed by replacing $r_0 \to r_{D1}$, $r_1 \to r_{D2}$, $k_1 \to k_D$ and $p_1 \to p_D = \sqrt{\varepsilon_D/\mu_D}$. Here r_{D1} and r_{D2} are the position interfaces of the defect layer, and k_d and p_d are wave vector associated with the defect layer and characteristic impedance of the defect layer, respectively. The component of the defect layer matrix can be written as $\hat{T}_D = \begin{bmatrix} t_{D11} & t_{D12} \\ t_{D21} & t_{D22} \end{bmatrix}$

$$t_{D11} = \frac{\pi}{2} k_D r_{D1} [Y_m'(k_D r_{D1}) J_m(k_D r_{D2}) - J_m'(k_D r_{D1}) Y_m(k_D r_{D2})], \tag{9a}$$

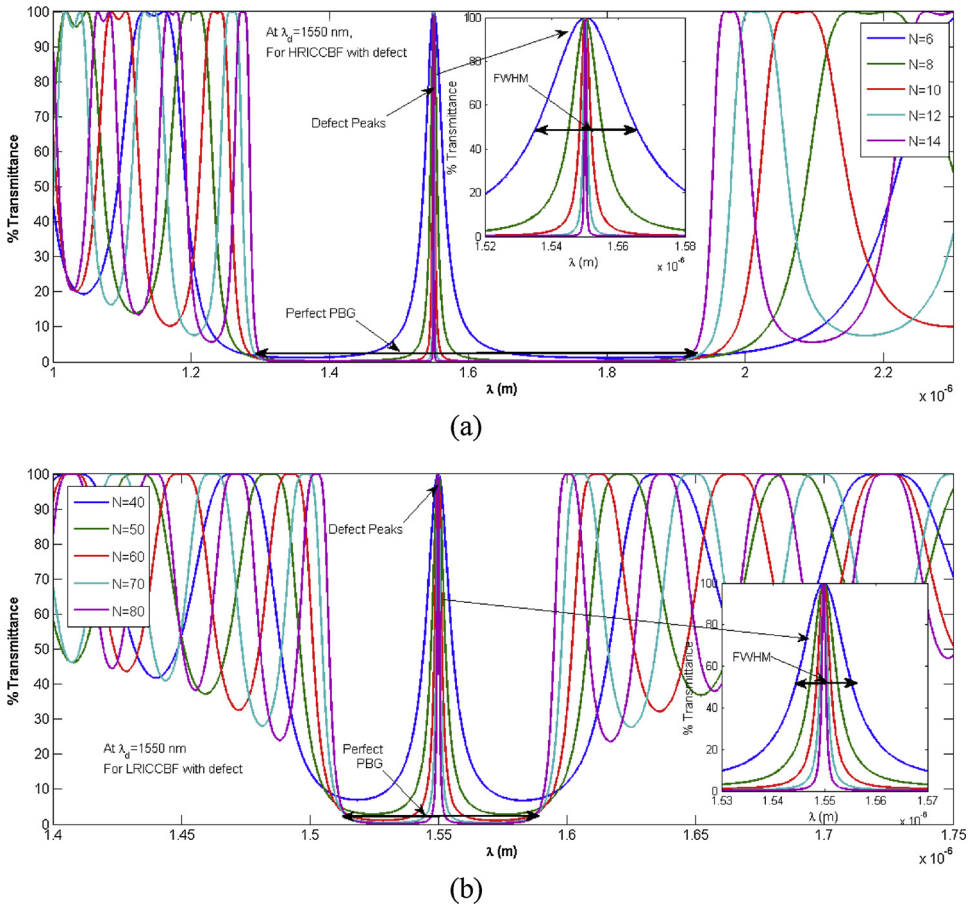

Fig. 2. Effect of number of cladding layers on FWHM of the defect peaks and photonic band gap at design wavelength *1550* nm for hollow core (a) HRICCBF (b) LRICCBF, and the design wavelength *632.8* nm for hollow core (c) HRICCBF (d) LRICCBF.

$$t_{D12} = j\frac{\pi}{2}\frac{k_D}{p_D} r_{D1}[J_m(k_D r_{D1})Y_m(k_D r_{D2}) - Y_m(k_D r_{D1})J_m(k_D r_{D2})], \tag{9b}$$

$$t_{D21} = -j\frac{\pi}{2} k_D r_{D1} p_D [Y_m^{'}(k_D r_{D1})J_m^{'}(k_D r_{D2}) - J_m^{'}(k_D r_{D1})Y_m^{'}(k_D r_{D2})], \tag{9c}$$

$$t^{D22} = \frac{\pi}{2} k_D r_{D1}[J_m(k_D r_{D1})Y_m^{'}(k_D r_{D2}) - Y_m(k_D r_{D1})J_m^{'}(k_D r_{D2})]. \tag{9d}$$

Thus, one can simply construct the matrix for all existing layers of multilayered Bragg fiber waveguide. The Bragg fiber waveguide structure total *2 N* numbers of matrices plus defect layer matrix are required to construct the total Transfer Matrix $\hat{T}$ that relates the first and final interfaces as

$$\begin{bmatrix} U(r_f) \\ V(r_f) \end{bmatrix} = \hat{T} \begin{bmatrix} U(r_0) \\ V(r_0) \end{bmatrix},$$

where

$$\hat{T} = \begin{bmatrix} T_{11} & T_{12} \\ T_{21} & T_{22} \end{bmatrix} = \hat{T}_{2N}\hat{T}_{2N-1}.....\hat{T}_{N+1}\widehat{T_D}\hat{T}_N.....\hat{T}_2\hat{T}_1. \tag{10}$$

With this calculated transfer matrix, the reflection and transmission coefficients can be determined through the fallowing relationships [17],

$$r_d = \frac{(T'_{21} + jp_0 C^{(2)}_{m0} T'_{11}) - jp_f C^{(2)}_{mf}(T'_{22} + jp_0 C^{(2)}_{m0} T'_{12})}{(-jp_0 C^{(1)}_{m0} T'_{11} - T'_{21}) - jp_f C^{(2)}_{mf}(-jp_0 C^{(1)}_{m0} T'_{12} - T'_{22})}, \tag{11}$$

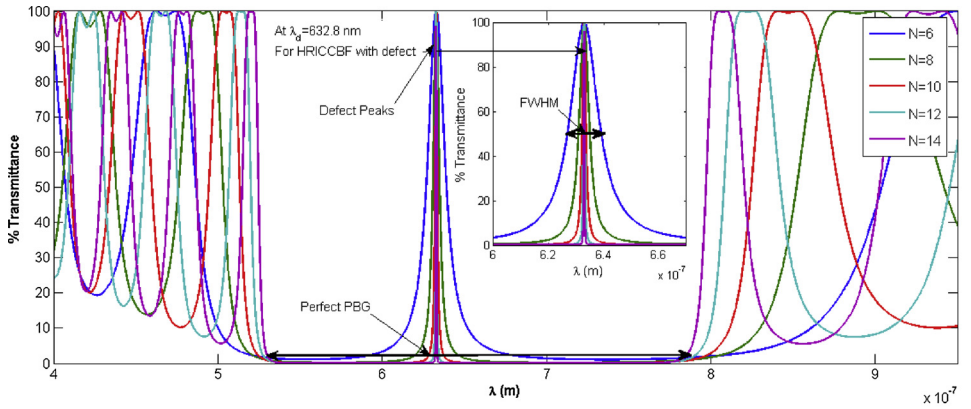

(c)

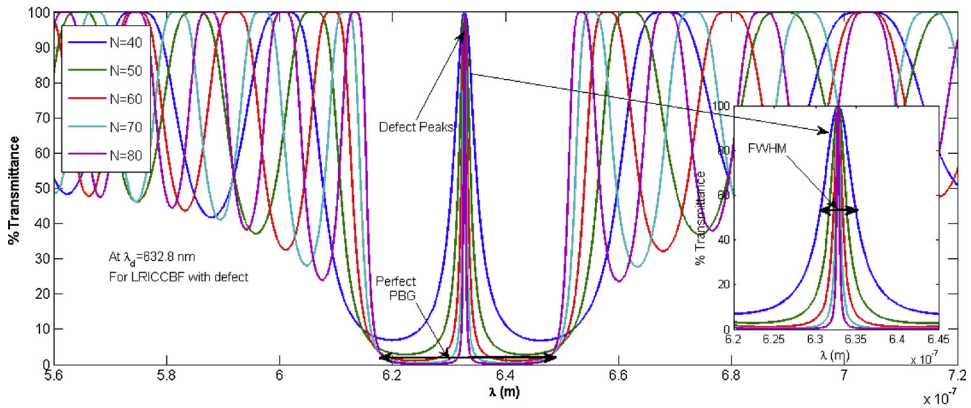

(d)

Fig. 2. (*continued*)

Table 1
Variation in FWHM and perfect photonic band gap (PPBG) with number of unit cell (N) in hollow core HRICCBF and LRICCBF with defect layer.

S. No.	HRICCBF with defect				LRICCBF with defect			
	At 1550 nm		At 632.8 nm		At 1550 nm		At 632.8 nm	
	N	FWHM(nm)	N	FWHM(nm)	N	FWHM(nm)	N	FWHM(nm)
1.	6	29.7	6	12.2	40	11.2	40	4.6
2.	8	9.8	8	3.9	50	5.6	50	2.3
3.	10	3.3	10	1.4	60	2.9	60	1.2
4.	12	1.0	12	0.5	70	1.6	70	0.6
5.	14	0.4	14	0.2	80	0.8	80	0.4

$$t_{\mathrm{d}} = \frac{4\sqrt{\varepsilon_0/\mu_0}}{\pi K r_0 H_{\mathrm{m}}^{(2)}(k_0 r_0) H_{\mathrm{m}}^{(1)}(k_0 r_0)[(-jp_0 C_{\mathrm{m0}}^{(1)} T_{11}' - T_{21}') - jp_{\mathrm{f}} C_{\mathrm{mf}}^{(2)}(-jp_0 C_{\mathrm{m0}}^{(1)} T_{12}' - T_{22}')]}, \tag{12}$$

where $p_0 = \sqrt{\varepsilon_0/\mu_0}$ and $p_{\mathrm{f}} = \sqrt{\varepsilon_{\mathrm{f}}/\mu_{\mathrm{f}}}$ are the admittance of core and final media, T_{11}', T_{12}', T_{21}' and T_{22}' are the matrix element of the inverse matrix of $\hat{T}$, $K = \omega\sqrt{\varepsilon_0\mu_0}$ is the free-space wave number and $C_{\mathrm{ml}}^{(1,2)} = \frac{H_{\mathrm{m}}^{(1,2)'}(k_1 r_1)}{H_{\mathrm{m}}^{(1,2)}(k_1 r_1)}$, $l = 0, f$.

where $H_m^{(1)}$ and $H_m^{(2)}$ are the Hankel function of the first and second kind. Using Eqs. (11) and (12), the percentage reflectance %R and Transmittance %T are:

$$\%R = 100 \times |r_{\mathrm{d}}|^2, \quad \%T = 100 \times \frac{n_{\mathrm{out}}}{n_{\mathrm{c}}} |t_{\mathrm{d}}|^2. \tag{13}$$

where n_{c} and n_{out} are the refractive indexes of the core and outer media.

The performance of proposed waveguide structures can be analyzed by using the various sensing parameters in which some

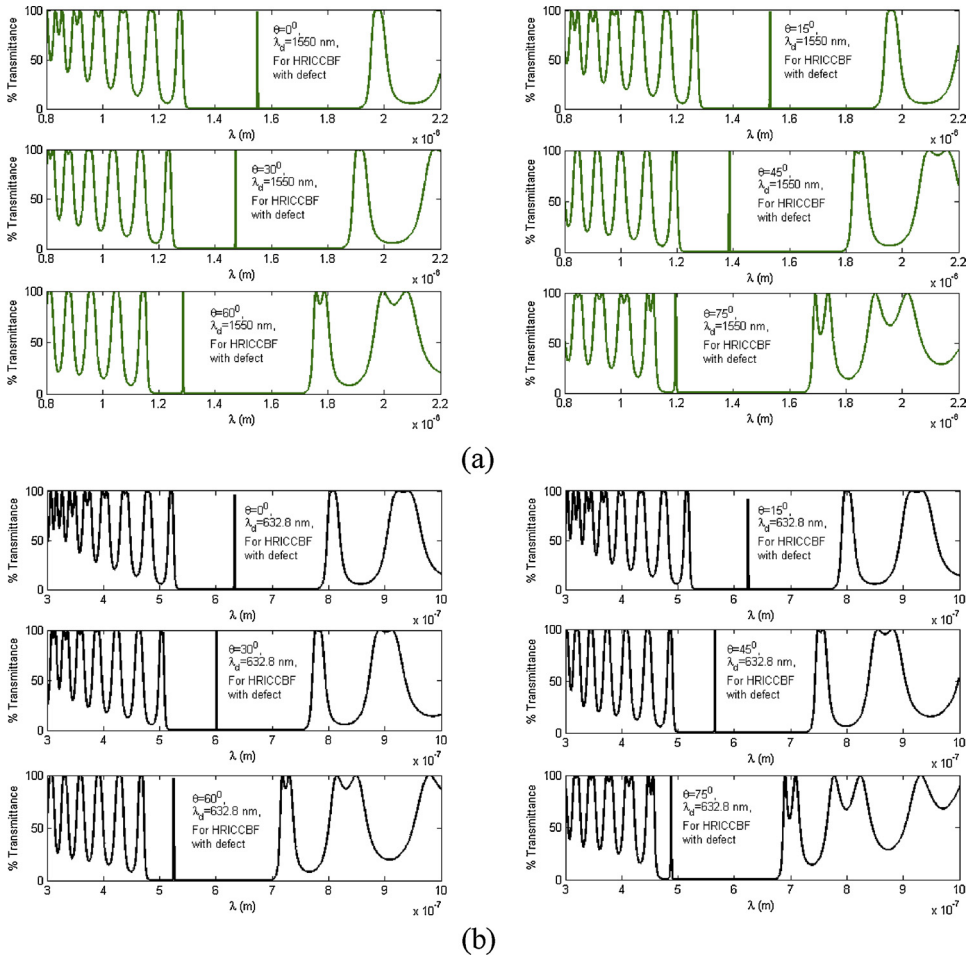

Fig. 3. Spectral shift of defect peak and obtained PPBG with angle of incidence in (a) HRICCBF waveguide at design wavelength *1550* nm, (b) HRICCBF waveguide at design wavelength *632.8* nm, (c) LRICCBF waveguide at design wavelength *1550* nm, (d) LRICCBF waveguide at design wavelength *632.8* nm.

important parameters are the sensitivity, detection accuracy and quality parameter. Sensitivity of sensor is defined by the ratio of the sensor measured output to the change in physical quantity to be measurend. Mathematically, sensitivity of sensor is defined as the ratio of spectral shift in resonance wavelength to the small change in aqueous medium or analyte refractive index present in core.

$$S = \Delta\lambda_{res}/\Delta n_c. \tag{14}$$

Detection accuracy describes the true value of the measurend. The detection accuracy of this sensor is the ratio of change in resonance wavelength with respect to the full width at half maximum (FWHM) of peak of defect mode. Quality parameter shows the overall performance of the sensor in terms of sensitivity and detection accuracy.

3. Results and discussion

Since, the spectral position of peak of defect mode strictly depend on spectral wavelength in which the operation takes place, therefore the propagation characteristic of both hollow core waveguides HRICCBF and LRICCBF with defect layer are studied in near infrared wavelength region having design wavelength λ_d = 1550nm and in visible region with design wavelength λ_d = 632.8nm. The fiber core and outer layer has to be taken air i.e. $n_c = n_{out} = 1.0$ and the core dimension has to be taken small enough $r_0 = 100(d_H + d_L)$ to avoid the losses occur due the presence of higher order modes. The bilayers cladding of hollow core HRICCBF waveguide is composed of high refractive index chalcogenide material (As_2Se_3) $n_H = 2.82$ and the low refractive index polymer material (PEI) $n_L = 1.66$ with a defect cavity in the mid of multilayer claddings [3,20] having thicknesses $d_H = \lambda_d/4n_H$, $d_L = \lambda_d/4n_L$ and $d_D = \lambda_d/4n_L$ which follow the quarter wave stack condition. Again, the bilayers cladding of hollow core LRICCBF waveguide is composed of high refractive index polymer material (PS) $n_H = 1.581$ and low refractive index polymer (PMMA) $n_L = 1.487$ with a defect cavity in the mid of multilayer claddings [4] having thicknesses which follow the same quarter wave stack condition as given above.

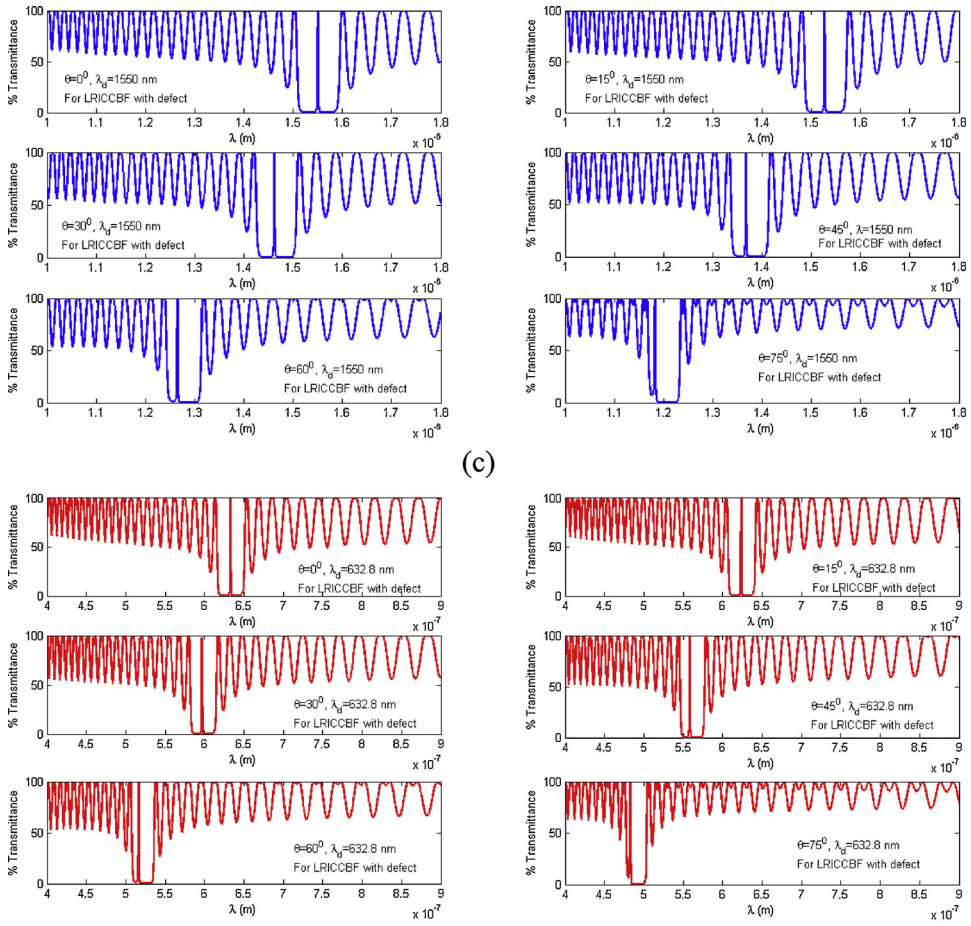

Fig. 3. (*continued*)

Table 2
Variation in the defect peak positions (DPP) and perfect photonic band gap (PPBG) with angle of incidence.

S. No.	HRICCBF with defect					LRICCBF with defect			
	At 1550 nm			At 632.8 nm		At 1550 nm		At 632.8 nm	
	θ°	DPP (nm)	PPBG (nm)	DPP (nm)	PPBG (nm)	DPP (nm)	PPBG (nm)	DPP (nm)	PPBG (nm)
1.	0	1550.0	634.0	632.8	258.6	1550.0	76.0	632.8	31.1
2.	15	1530.0	629.0	624.6	256.6	1527.0	75.0	623.3	30.7
3.	30	1472.0	613.0	600.8	250.2	1461.0	72.0	596.7	29.3
4.	45	1385.0	589.0	565.6	240.5	1367.0	67.0	558.1	27.3
5.	60	1286.0	561.0	525.0	228.9	1265.0	61.0	516.3	25.0
6.	75	1195.0	528.0	487.8	215.4	1183.0	60.0	482.7	24.3

Fig. 2 shows the existence of perfect photonic band gap (PPBG) in both considered waveguide structures at both design wavelengths. The PPBG is the range of wavelength having 0% transmittance. Fig. 2(a) and (b) show the variation of % transmittance with the wavelength of incidence light for respective hollow core HRICCBF and LRICCBF with defect cavity at design wavelength *1550* nm. The obtained PPBG for hollow core HRICCBF is (*635* nm) in Fig. 2(a) due to its strong reflectivity in comparison to the hollow core LRICCBF (*76* nm) in Fig. 2(b). Again, Fig. 2(c) and (d) show the transmittance of hollow core HRICCBF and LRICCBF waveguides with defect cavity at design wavelength *632.8* nm. It is clear that the obtained PPBG for HRICCBF (*259* nm) and LRICCBF (*31* nm) decreases with decrease of design wavelength. The obtained PPBG in HRICCBF waveguide is always larger than the LRICCBF at considered designed wavelengths. It is also clear from these figures that in hollow core HRICCBF only few numbers of cladding layers (N = 14) are sufficient to provide the PPBG while in hollow core LRICCBF to obtained PPBG large number of cladding layers

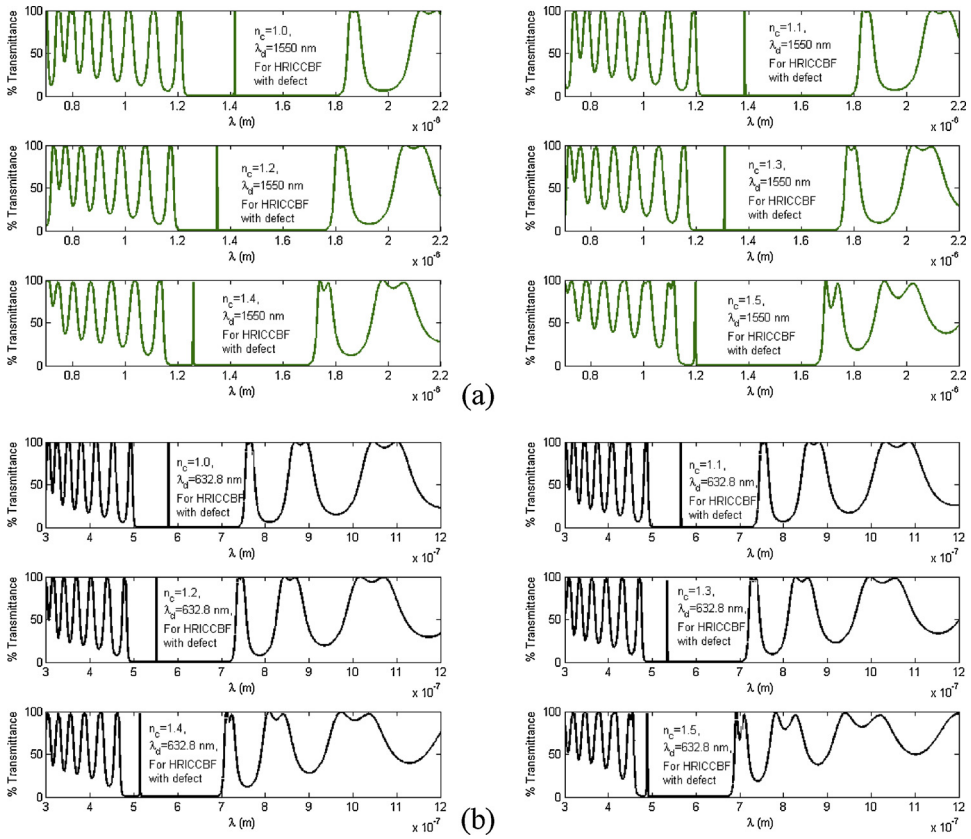

Fig. 4. Variation in photonic band with core refractive indices in (a) HRICCBF waveguide at design wavelength *1550* nm, (b) HRICCBF waveguide at design wavelength *632.8* nm,(c) LRICCBF waveguide at design wavelength *1550* nm, (d) LRICCBF waveguide at design wavelength *632.8* nm.

(N = 80) are required. In addition to this, the presence of defect cavity in such waveguides provides a very sharp pass band in PPBG region with almost 100% transmittance due to existence of the Febry-Perot resonant condition. The FWHM of this sharp pass band gradually decreases with increase of cladding period *N*, which is tabulated in Table 1. The small value of FWHM enhances the sensing performance of Bragg fiber sensor and also increases the quality parameter of the inline Bragg filter beam. From above discussion, it is observed that the PPBG of the proposed structure is highly depend on the contrast of refractive indices of used materials and decreases with decrease of refractive index contrast, also the position and size of band gap does not depend on number of layers but the FWHM of the peak of defect mode is strictly depend on the number of periodic bilayers.

In order to see the effect of various incidence angle of electromagnetic wave on PPBG, 14 number of unit cells are taken in hollow core HRICCBF waveguide and 80 number of unit cells are taken in hollow core LRICCBF waveguide. The spectrum of PPBG and shift in peak of defect at different angle of incidence are shown in Fig. 3. Fig. 3(a), (b) and (c), (d) show the respective position of peak of defect mode and the PPBG at two considered design wavelengths 1550 nm and 632.8 nm for hollow core HRICCBF and LRICCBF waveguides. From these figures, positions of peak of defect mode and PPBG are calculated and tabulated in Table 2. It is clear from Table 2 that the change in angle of incidence from 0^0 to 75^0, able to shift in peak of defect mode 355 nm and PPBG 106 nm for design wavelength 1550 nm but comparatively provide small shift in peak of defect mode 145 nm and PPBG 43.2 nm for design wavelength 632.8 nm in hollow core HRICCBF waveguide. Similarly, in hollow core LRICCBF waveguide for the same change in angle of incidence able to shift in peak of defect mode position 367.0 nm and 150.1 nm and change in PPBG 16.0 nm and 6.8 nm for respective design wavelengths 1550 nm and 632.8 nm. Finally, from Table 2 the obtained photonic band gaps for both design wavelengths decreases with increase the incidence angle of light. These decrease of photonic band gap with incidence angles are observed due to decrease in geometrical path of light. Also, the peaks of defect mode are blue shifted with decrease of geometrical path of light.

These hollow cores Bragg fiber waveguides structure with defect cavity can be used for chemical and bio-sensing application by assuming the defect peak present in the PPBG as a sensing signal. In order to estimate the bio-sensing application of these waveguides the variation in defect peak position with core refractive indices in both HRICCBF and LRICCBF waveguides at both considered design wavelengths at $\theta^0 = 40^0$ are plotted in Fig. 4 and tabulated in Table 3. It is clear from Table 3, that for sensing application one can monitor spectral shift of peak of defect mode present in the PPBG. The obtained sensitivities by measuring the spectral shift of peak of defect mode for HRICCBF waveguide are 440.0 nm/RIU and 179.2 nm/RIU at respective design wavelengths 1550 nm and 632.8 nm. These sensitivities for LRICCBF waveguide are 434.0 nm/RIU and 177.2 nm/RIU at same respective design wavelengths 1550 nm and 632.8 nm. However, the other sensing parameters like detection accuracy, quality parameter highly depend on the FWHM value of

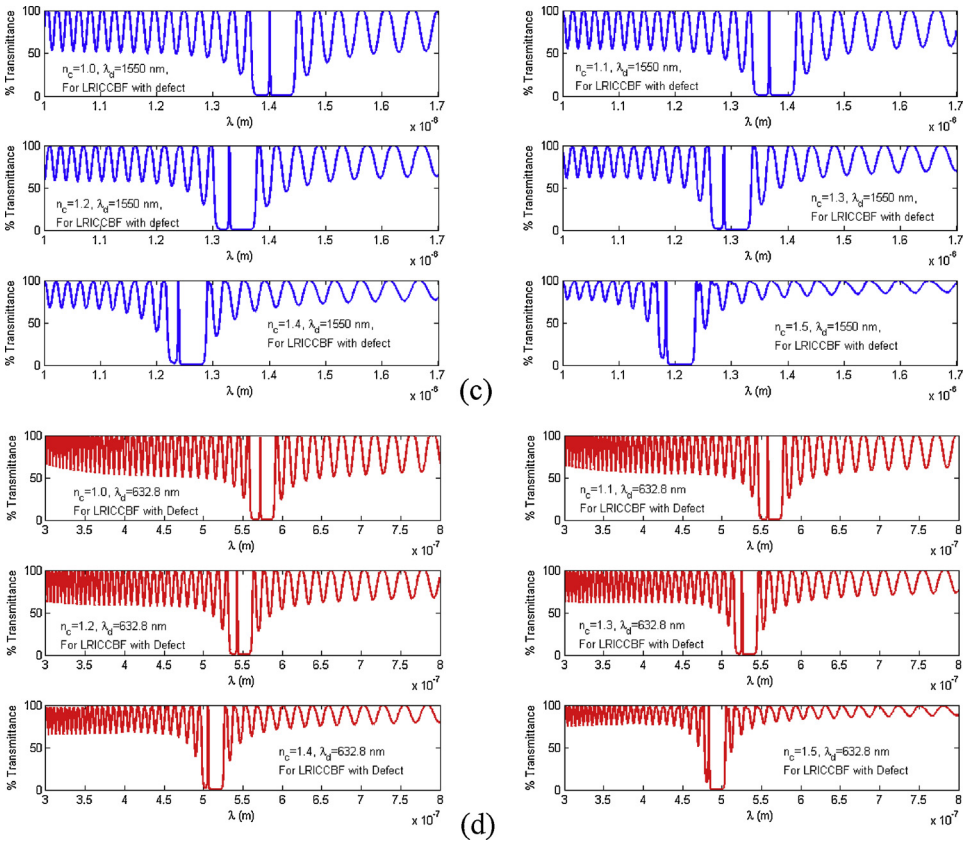

Fig. 4. (*continued*)

Table 3
Variation in the defect peak positions (DPP) and perfect photonic band gap (PPBG) with core refractive index.

S. No.	HRICCBF with defect					LRICCBF with defect			
	At 1550 nm			At 632.8 nm		At 1550 nm		At 632.8 nm	
	n_c	DPP (nm)	PPBG (nm)	DPP (nm)	PPBG (nm)	DPP (nm)	PPBG (nm)	DPP (nm)	PPBG (nm)
1.	1.0	1417.0	658.0	578.3	244.1	1401.0	69.0	571.9	28.2
2.	1.1	1385.0	589.0	565.6	240.5	1367.0	67.0	558.1	27.4
3.	1.2	1350.0	578.0	551.0	236.3	1329.0	65.0	542.7	26.6
4.	1.3	1308.0	566.0	534.1	231.3	1287.0	63.0	525.3	25.4
5.	1.4	1259.0	551.0	514.0	225.0	1239.0	61.0	505.6	24.7
6.	1.5	1197.0	526.0	488.7	215.7	1184.0	60.0	483.3	23.6

the sensing signal. It is clear from Fig. 2 that, the FWHM of peak of defect mode is much smaller than the FWHM of the PPBG, therefore these parameters have large values when one use of peak of defect mode as sensing signal. Hence, it is found that the monitoring of peak of defect mode instead of monitoring PBG will provide better detection accuracy and quality parameter of the sensor systems. Also, the FWHM of the peak of defect mode is small in LRICCBF waveguide with the respective FWHM of HRICCBF waveguide. Therefore, for sensing application LRICCBF waveguide with defect mode is recommended.

4. Conclusions

A high contrast HRICCBF and a low contrast LRICCBF hollow core waveguides having a defect layer are studied and compared at two designed wavelengths. In comparison to LRICCBF waveguide, lower number of periodicity is required to obtain PPBG in HRICCBF. The FWHM of defect peak decreases with increase of periodicity of cladding layers in both considered waveguides. The shift in peak of defect mode positions and perfect photonic band gap with angle of incidence or the variation of core RI, for HRICCBF is always larger than the LRICCBF at respective deign wavelength. Hence, the obtained sensitivity for HRICCBF is always larger than

LRICCBF waveguide but the same time the FWHM of defect peak in LRICCBF waveguide at a design wavelength is much smaller than the respective HRICCBF waveguide therefore the overall quality parameter in LRICCBF is improved considerably.

Declaration of Competing Interest

No Conflict of interest.

Acknowledgments

Chandan Singh Yadav and Abhishek Upadhyay acknowledge DST and UGC for finential assistence.

References

[1] P. Yeh, A. Yariv, Bragg reflection waveguides, Opt. Commun. 19 (1976) 427–430.
[2] B. Temelkuran, S.D. Hart, G. Benoit, J.D. Joannopoulos, Y. Fink, Wavelength scalable hollow optical fibers with large photonic bandgaps for CO2 laser transmission, Nature 420 (2002) 650–653.
[3] K.J. Rowland, V.S. Afshar, A. Stolyarov, Y. Fink, T.M. Monro, Bragg waveguides with low index liquid cores, Opt. Express 20 (2011) 48–62.
[4] Q. Hang, M. Skorobogatiy, Resonant bio-and chemical sensors using low-refractive index contrast liquid-core Bragg fibers, Sens. Actuators B 161 (2012) 261–268.
[5] L. Shi, W. Zhang, J. Jin, Y.D. Huang, J.D. Peng, Hollow core Bragg fiber and it application in trace gas sensing, Communications and Photonics Conference and Exhibition (ACP) Asia, IEEE Xplore (2010), https://doi.org/10.1109/ACP.2010.5682586.
[6] Q. Hang, T. Brastaviceanu, F. Bergeron, J. Olesik, I. Pavlov, T. Ishigure, M. Skorobogatiy, Photonic bandgap Bragg fiber sensors for banding/displacement detection, Appl. Opt. 52 (2013) 6344–6349.
[7] H.A. Elsayed, A. Mehaney, New method for glucose detection using the one dimensional defective photonic crystals, Mater. Res. Express 6 (2019) 036201.
[8] G. Sharma, S. Kumar, S. Prasad, V. Singh, Theoretical modeling of one dimensional photonic crystal based optical de-multiplexer, J. Mod. Opt. 63 (2016) 995–999.
[9] A. Al-Juboori, P.J. Reece, Extending omnidirectional reflection bands in one-dimensional photonic crystals, J. Phys. Commun. 2 (2018) 055003.
[10] G. Vienne, Y. Xu, C. Jakobsen, H.J. Deyerl, J. Jensen, T. Sorensen, T. Hansen, Y. Huang, M. Terrel, R. Lee, N. Mortensen, J. broeng, H. Simonsen, A. Bjarklev, A. Yariv, Ultra large bandwidth hollow guiding in all silica Bragg fibers with nano supports, Opt. Express 12 (2004) 3500–3508.
[11] S. Golmohammadi, Y. Rouhani, K. Abbasian, A. Rostami, Photonic bandgaps in quasiperiodic multilayer using Fourier transform of the refractive index profile, PIER B 5 (2008) 133–152.
[12] Q. Wang, X. Wang, L. Zhang, Y. Wang, W. Qiao, X. Han, X. Cai, W. Yu, Dimensional photonic crystals containing a Dirac semimetal-based metamaterial defect layer, Appl. Opt. 58 (2019) 94–101.
[13] L. González-García, S. Colodrero, H. Míguez, A.R. González-Elipe, Single-step fabrication process of 1-D photonic crystals coupled to nanocolumnar TiO2 layers to improve DSC efficiency, Opt. Express 23 (2015) A1642–A1650.
[14] R.K. Chourasia, V. Singh, Estimation of photonic band gap in the hollow core cylindrical multilayer structure, Superlatt. Microstruct. 116 (2018) 191–199.
[15] Y. Gao, N. Guo, B. Gauvreau, M. Rajabian, O. Skorobogata, E. Pone, O. Zabeida, L. Martinu, C. Dubois, M. Skorobogatiy, Consecutive solvent evaporation and co-rolling techniques for polymer multilayer hollow fiber perform fabrication, J. Mater. Res. 21 (2006) 2246–2254.
[16] E. Pone, C. Dubois, N. Guo, Y. Gao, A. Dupuis, F. Boismenu, S. Lacroix, M. Skorobogatiy, Drawing of the hollow all-polymer Bragg fibers, Opt. Express 14 (2006) 5838–5852.
[17] M.A. Kaliteevski, R.A. Abram, V.V. Nikolaev, G.S. Sokolovski, Bragg reflectors for cylindrical waves, J. Mod. Opt. 46 (1999) 875–890.
[18] A.H. Cherin, An Introduction to Optical Fibers, Mc Graw-Hill International, Tokyo, 1983.
[19] M. Born, E. Wolf, Principles of Optics, Cambridge, London (1999).
[20] K. Kuriki, O. Shapira, S.D. Hart, G. Benoit, Y. Kuriki, J.F. Viens, M. Bayindir, J.D. Joannopoulos, Y. Fink, Hollow multilayer photonic bandgap fibers for NIR applications, Opt. Express 12 (2004) 1510–1517.